Rasayely
Membrane Science International
https://rasayely-journals.com/index.php/msi
Vol 4(1);1–11, 2025

Original Article Open Access

Enhanced Filtration Performance of Hollow Fiber PVDF Membranes with Selective Pore Size Control via Modified NIPS Method

Nikita Fateev[1,*], Klim Velmozhin[1], Andrey Danilkin[1], Anna Kotyukova[1], Tatiana Yasneva[1], Mikhail Ivanov[2], and George Kagramanov[2]

[1]*TECON Membrane Technologies LLC, Moscow 123298, Russia*
[2]*D. Mendeleev University of Chemical Technology of Russia, Moscow 125047, Russia*

[*]Author to whom any correspondence should be addressed; Email: fateev@tecon.ru

Received: 05 March 2025; Revised: 30 June 2025; Accepted: 23 July 2025; Published: 30 August 2025

Academic Editor: Hao-Cheng Yang, Sun Yat-sen University, China

Abstract

The production of PVDF hollow fiber membranes via the non-solvent induced phase separation (NIPS) method is one of the most straightforward and cost-effective techniques. However, conventional NIPS processes often struggle to achieve a narrow pore size distribution, limiting their performance in precision ultrafiltration applications. In this work, we present an enhanced NIPS approach that enables fine control over the membrane's limiting pore size. By carefully tuning the composition of the spinning solution and optimizing processing parameters, we achieved precise regulation of membrane structure. The resulting membranes exhibited a wide range of well-defined limiting pore sizes—from 80 nm, offering high water permeability (960 $L \cdot m^{-2} \cdot h^{-1} \cdot bar^{-1}$), down to 10 nm with lower permeability (68 $L \cdot m^{-2} \cdot h^{-1} \cdot bar^{-1}$). These findings demonstrate the versatility and tunability of the modified NIPS method, enabling the fabrication of PVDF membranes tailored for specific ultrafiltration applications.

Keywords

Ultrafiltration; hollow fiber; membrane; PVDF; NIPS; permeability; block copolymers

1. Introduction

Polyvinylidene fluoride (PVDF) has long been recognized as a preferred material for membrane fabrication due to its widespread commercial availability, exceptional chemical and thermal stability, and superior mechanical properties. This polymer exhibits good solubility in a range of classical organic solvents, including *N,N*-dimethylacetamide (DMAc), 1-methyl-2-pyrrolidinone (NMP), *N,N*-dimethylformamide (DMF), triethyl phosphate (TEP), and dimethyl sulfoxide (DMSO), among others [1].

For water treatment applications, PVDF is commonly used in the production of hollow fiber membranes with an external selective layer, typically designed for ultrafiltration and microfiltration. The hollow fiber configuration offers a large active surface area, which directly contributes to improved membrane element performance [2].

Despite its many advantages, the use of PVDF membranes in water treatment is often limited by their inherent hydrophobicity. This characteristic leads to relatively low water flux, increased fouling, and reduced backwash efficiency [3]. However, PVDF membranes' high elongation at break, combined with the external selective layer, allows for the incorporation of alternative cleaning methods, such as air purging and mechanical scrubbing using air bubbles under pressure. These methods, which involve the movement of air parallel to the membrane surface, help mitigate fouling and reduce operational costs, particularly in ultrafiltration and microfiltration systems [4]. As a result, PVDF-based membranes, along with PES-based membranes, remain domi-

nant in the field of water treatment, providing a cost-effective solution with enhanced cleaning capabilities.

PVDF membranes are currently produced using two primary methods: phase separation induced by the interaction with a non-solvent (typically water) and thermally induced phase separation (TIPS) [5]. Each method has distinct advantages and limitations. Membranes produced via the TIPS method are often characterized by superior mechanical properties, a narrower pore size distribution, and enhanced control over morphology, allowing for the formation of the desired spongy structure. However, the TIPS process requires more complex equipment and higher energy consumption to maintain elevated processing temperatures (up to 200 °C). In contrast, membranes produced by the non-solvent induced phase separation (NIPS) method utilize simpler equipment and operate at lower energy costs, making it a more cost-effective approach. Additionally, membranes fabricated by the NIPS method tend to exhibit better antifouling properties, which is particularly advantageous in water treatment applications [6].

This study focuses on the fabrication of PVDF membranes using the NIPS method, with particular attention given to addressing the inherent challenges associated with this process. A primary issue is the low hydrophilicity of PVDF, which limits its effectiveness for water treatment applications. To mitigate this, pore-forming agents and hydrophilic molecules are incorporated into the casting solution, which helps to concentrate at the phase separation boundary and enhancing the overall hydrophilicity of the resulting membrane. Key additives include amphiphilic and hydrophilic polymers such as polyvinylpyrrolidone (PVP), polyethylene glycol (PEG), and Pluronic®-type block copolymers. Additionally, metal salts (e.g., lithium chloride, calcium chloride, lithium perchlorate), ceramic particles (e.g., TiO_2, Al_2O_3, ZrO_2), and surfactants (e.g., Triton X-100, Span 80, Tween 20) are commonly incorporated to enhance membrane characteristics [7]. For instance, an increase in membrane flux was observed upon adding lithium chloride and PVP with a molecular weight (Mw) of 10K to the casting solution [8]. it has been reported that the properties of the resulting membranes are influenced by the molecular weight of PVP in the spinning solution [9]. Similarly, the impact of Tween 20 surfactant on membrane morphology has been demonstrated, noting its ability to improve the pore distribution and surface characteristics [10]. In addition, the significant effect of TiO_2 particles in the casting solution on membrane performance has been highlighted, with the incorporation of TiO_2 particles shown to enhance membrane permeability [11]. Furthermore, TiO_2 particles have been shown to contribute to the membrane's antifouling properties by reducing the accumulation of organic and inorganic fouling agents on the membrane surface, thereby extending its operational lifespan [11].

In the context of a patent by LOTTE CHEMICAL CORPORATION (US 2018/0085715 A1), a PVDF membrane containing small amounts of acetylated methyl cellulose was characterized, which was shown to improve the mechanical and antifouling properties of the membrane [12]. Further, an in-depth analysis has been provided regarding the effects of Pluronic F127 on membrane quality, particularly its influence on pore structure and surface morphology [13]. In addition to the use of additives, some studies have explored post-formation modifications to improve membrane properties. Techniques such as UV treatment, plasma treatment, and other surface modification methods have been investigated to enhance the hydrophilicity, antifouling performance, and selectivity of the membranes [7].

Another significant challenge in NIPS-based membrane fabrication is achieving a regular spongy structure and a narrow pore size distribution in the selective layer. This is influenced by several factors during the membrane formation process, including the composition of the casting solution (e.g., molecular weight and concentration of PVDF, solvent nature, and the presence of additives), spinning parameters (such as temperature, bore composition, take-up speed, coagulation bath composition, and air gap height), as well as post-processing conditions [14]. The rate of phase separation plays a crucial role in determining the structure of the final membrane. Rapid phase separation, where the solvent quickly exchanges with water, tends to form membranes with macrovoids. In contrast, slower phase separation, which can be achieved by adding precipitants to the spinning solution or by increasing the softness of the coagulation bath, facilitates the formation of a more uniform spongy structure [15]. Fine-tuning these factors is essential for controlling the pore size distribution and achieving the desired membrane morphology, which is critical for optimizing filtration performance.

The choice of solvent for the polymer is a critical step in the production of the spinning solution for membrane fabrication. The solvent not only influences the physical properties of the solution, such as density and viscosity, but also plays a key role in the diffusion rate into water and its solubility with respect to the polymer. It has been demonstrated that the use of triethyl phosphate (TEP) as a solvent in the spinning solution, which has a relatively low solvent capacity for PVDF and a slow diffusion rate into water, results in the formation of a regular spongy membrane structure [7].

It has been emphasized that increasing the softness of the coagulation bath, or bore fluid, positively influences membrane morphology and concentricity [16]. It has also been shown that the impact of the coagulation bath composition on membrane characteristics reinforces the significance of bath parameters in determining the final membrane structure and performance [17].

In this study, we aimed to fabricate an ultrafiltration hollow fiber membrane made of PVDF using the NIPS method, targeting high permeability values while maintaining a regular sponge structure without macrovoids. Additionally, we sought to explore the main factors influencing membrane performance. It is important to note that the membrane production method employed here is not purely NIPS. Phase separation begins in the air gap of the precipitation bath, where the presence of water vapor significantly contributes to the formation of the outer selective layer [18]. In this process, the temperature of the polymer solution is maintained at 90°C, and the solution cools in the spinneret, approaching the gelation point. As a result, the method can be characterized as a hybrid approach combining NIPS with elements of VIPS (Vapor-Induced Phase Separation) and TIPS (Ther-

mally Induced Phase Separation). This approach allows for greater control over membrane morphology, contributing to the achievement of the desired membrane structure and performance characteristics.

2. Methods and Materials

2.1. Materials

The following materials were used in this study: polyvinylidene difluoride (PVDF) KYNAR® G150 (Arkema, France); polyvinylidene difluoride (PVDF) Solef® 6008 (Solvay, Belgium); polyvinylpyrrolidone (PVP) K90 WIRUD (Mw = 1400 kDa, WIRUD GmbH, Germany); glycerol (≥ 99.5%, AKRIHIM, Russia); dimethylformamide (DMF, ≥ 99.0%, Shandong Hualu-Hengsheng Chemical Co., Ltd, China); dimethyl sulfoxide (DMSO, ≥ 99.0%, Shandong Hualu-Hengsheng Chemical Co., Ltd, China); lyophilized myoglobin from equine skeletal muscle (≥ 96%, Solarbio, China); bovine serum albumin (≥ 97%, Solarbio, China); lithium chloride (≥ 99%, Jinan Sintop Co., China); and sodium chloride (≥ 99%, Jinan Sintop Co., China).

2.2. Methods

2.2.1. Scanning Electron Microscopy Method

The analysis was performed using a Helios NanoLab™ 600i (USA) scanning probe microscope in tapping mode. Wet membrane samples were rapidly frozen in liquid nitrogen and then fractured to obtain cross-sections. The samples were subsequently dried overnight. Surface samples were coated for 30 seconds, and cross-sectional samples for 45 seconds, with a gold–platinum alloy using an Emitech SC7620 sputtering machine. Pore sizes were analyzed using ImageJ 1.41 software (National Institutes of Health, Bethesda, Maryland, USA), calculating the average pore size and standard deviation for each size distribution. The average membrane thickness was measured at five different locations on each sample using a Mitutoyo digital micrometer (Mississauga, Ontario, Canada).

2.2.2. Pore Size Distribution

A standard bubble point test was conducted to assess the integrity of the membrane. This method, widely used by membrane manufacturers globally, is described in greater detail in other publications **[19,20]**. In this procedure, a 5-meter-long membrane fiber was immersed in water, and compressed nitrogen was introduced into the fiber. The pressure was gradually increased until the membrane surface began to bubble.

However, this method is relatively crude. It cannot provide detailed information on the distribution of pores in the membrane and only serves to confirm the absence of significant structural defects.

To better characterize the pores, we employed the Liquid–Liquid Displacement Porosimetry (LLDP) method. For this purpose, we used the POROLIQ™ 1000 SERIES porometer, which is detailed in other specialized studies **[19,20]**. LLDP involves two immiscible liquids. One liquid, referred to as the wetting liquid, is chosen for its high affinity to the membrane material, ensuring complete wetting and filling of all the pores. The second liquid, called the displacing liquid, has a lower affinity and is used to displace the wetting liquid **[20]**.

Pore size is determined based on the applied pressure, which is a function of the interfacial tension between the two liquids. This method assumes that the pores are cylindrical and unevenly distributed. The pressure (ΔP) required to force the displacing liquid into a pore filled with wetting liquid is described by the Young–Laplace equation **[19]**. For this analysis, we selected a liquid pair; water as the wetting liquid and isobutanol as the displacing liquid.

2.2.3. Organic Molecules Cut-Off and Permeability Test

A laboratory-scale experimental setup was used to evaluate the performance of the membrane **(Figure 1)**. The test module consisted of a steel tube with an outer diameter (OD) of 15 mm and an inner diameter (ID) of 12 mm, housing 10 hollow fiber membranes, each with an effective length of 40 cm. The experiments were conducted with wet hollow fiber membranes.

A 0.1 M NaCl aqueous solution containing myoglobin and albumin **(Table 1)** was used as the feed solution, which was introduced into the inter-fiber space at a pressure of 2 bar.

The system was configured using ball valves and a feed pump to ensure that 10% of the initial flow was directed to the permeate and 90% to the retentate. The concentrations of myoglobin and albumin in the feed (C_f) and permeate (C_p) solutions were determined using a Roche Cobas 8000 analyzer (Switzerland). The rejection of myoglobin and albumin (R_s) was calculated using the following formula:

$$R_s = \left(1 - \frac{C_p}{C_f}\right) \times 100\% \qquad (1)$$

Fiber permeability was measured on individual fiber samples with a length of 50 cm. A schematic representation of the experimental setup is standard and commonly described in other studies **[16]**. The measurements were conducted at a pressure drop of 1 bar using prepared reverse osmosis water in dead-end mode. Water was supplied to the outside of the membrane sample. Permeability was calculated using the following formula:

$$Lp_{TMP} = \frac{V_p}{\pi * dext * l * t * TMP} * (0.0006533 * T^2 - 0.0559 * T + 1.865) \quad (2)$$

Where Lp_{TMP} is the membrane permeability ($L.m^{-2}.h^{-1}.bar^{-1}$), measured in outside-in mode at a specific TMP (bar), d_{ext} is the external diameter (m) and l is the length (m) of the hollow fiber membrane sample, t (h) is the time it takes for a certain amount of permeate Vp (l) to pass through membrane sample, and *T* is temperature (°C).

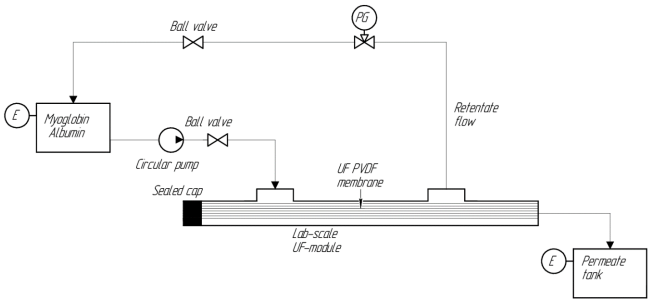

Figure 1: Organic molecules cut-off test system.

Table 1: Composition of the initial cut-off solution.

№	Component	Concentration, g/L
1	Myoglobin	5×10^{-5}
2	Albumin	5
3	Sodium chloride	6

3. Results and Discussion

3.1. Spinning Solution

The choice of spinning solution significantly influences the final properties of the membrane. The literature provides numerous examples of spinning solutions and their additives for the preparation of UV PVDF membranes. In this study, we focused on the key components that are expected to have the greatest impact on the final characteristics of the membrane.

The concentration of PVDF in all solutions was fixed at 18%, which is sufficient to ensure the mechanical integrity of the final membrane. Two different grades of PVDF were employed in this study: one with a higher molecular weight (Kynar® G150) and the other with a lower molecular weight (Solef® 6008) **[21]**. The inclusion of the lower molecular weight PVDF was intended to reduce the solution viscosity. Previous research has shown that using a PVDF mixture in membrane spinning results in a smoother surface and enhanced permeability **[22]**. However, at higher concentrations of Solef® 6008, macrovoids began to form within the membrane structure. The maximum permissible concentration of Solef® 6008 in the PVDF mixture, at which macrovoids were absent, was determined **(Figure 2)**. At a PVDF ratio of 9:9, single macrovoids were already observed, prompting the incorporation of Kynar® G150 at a concentration of 12%, while Solef® 6008 was used at 6%.

Dimethyl sulfoxide (DMSO) and dimethylformamide (DMF) were used as solvents in this study. DMSO is a safe, polar aprotic solvent often classified as a "green" solvent. However, PVDF solutions in DMSO exhibit a high dynamic viscosity (1.9 MPa·sec), which limits their use. To overcome this limitation, DMF, with a lower dynamic viscosity of 0.9 MPa·sec, was used as a co-solvent **[23]**.

To promote phase separation and prevent the formation of macrovoids, reverse osmosis water was added as a non-solvent. Water is a strong precipitant for PVDF and effectively shifts the solution equilibrium toward the binodal line. Consequently, only small amounts of water were required in the spinning solution.

Lithium chloride (LiCl) was used as a pore-forming agent, maintaining a consistent concentration of 5% in all spinning solutions, as suggested by prior research. In addition, polyvinylpyrrolidone (PVP K-90) was introduced to enhance the hydrophilicity of the membrane and to act as a secondary pore-forming agent **[8,24]**. The hydrophilic nature of PVP increases the water sorption capacity of the membrane. It was observed that PVP was distributed unevenly within the membrane structure during formation, with its concentration increasing from the center of the membrane wall toward the surface **[25]**. Due to its high molecular weight, PVP K-90 is not fully removed during the membrane fabrication process and remains embedded within the membrane matrix.

It was found that an increase in the molecular weight of PVP in the spinning solution suppressed macrovoid formation, leading to an increase in both the number of pores and the overall porosity of the membrane **[26]**. Similarly, it was reported that in standard systems consisting of a polymer, polar aprotic solvent, and water, higher concentrations of PVP in the solution inhibited macrovoid formation by slowing down the phase separation process **[27]**.

Amphiphilic Polyarylate-polyalkylene oxide (PAR-PAO) block copolymers synthesized earlier were also added to the polymer composition. Polymers of this type are hydrophilic, but at the same time insoluble in water due to the terephthalic fragment, which serves as a kind of anchor that retains the polymer molecule on the membrane surface **[28]**. Therefore, it was assumed that the pore size of the selective membrane layer could be controlled. The compositions of the polymer solutions are presented in **Table 2**.

For each solution, viscosity was measured using an A&D SV 100 viscosity analyzer (Japan). All viscosity values were recorded at 60°C **(Table 3)**. This temperature was chosen because PVDF is a semi-crystalline polymer that tends to gel. Gelation refers to a special state where the solution loses its ability to flow and transforms into a so-called "soft solid" **[29]**. Gels are formed when polymer chains crosslink, creating a three-dimensional network that traps a significant amount of solvent. This phenomenon is commonly observed in solvents containing a ketone group (e.g., cyclohexanone-γ-butyrolactone). However, such behavior was not observed in PVDF solvents without ketone fragments (e.g., DMAc, DMF, and DMSO) **[23]**. Nonetheless, at high PVDF concentrations and in the presence of PVP, gelation of the polymer solutions was observed.

The gelation temperature of each solution was measured. For these polymer solutions, the classical turbidity point was not observable. The binodal line, or liquid–liquid phase separation line, is located below the gelation temperature. As a result, the crystallization of PVDF prevents the accurate identification of the binodal line using haze points **[30]**. During the non-solvent-induced phase separation (NIPS) process, membrane formation does not solely follow the

classical liquid–liquid phase separation (LLPS) mechanism. Instead, PVDF may undergo deposition through either LLPS or gelation caused by crystallization, leading to solid–liquid (S–L) phase separation. It is well known that PVDF crystals can adopt three different molecular conformations: trans–gauche–trans–gauche' (TGTG'), trans–trans–trans (TTT), and trans–trans–trans–gauche (TTTG) [23]. Therefore, the intersection of the gelation temperature of the polymer solution provides an additional method to control the properties of the membrane [30].

3.2. Membrane Spinning

The hollow fiber membrane was prepared using a lab-scale manufacturing line, as previously described in the literature [31]. The reactors for the polymer solution and bore solution were equipped with jacketed silicone heating. The polymer and bore solutions were delivered to the spinneret using gear pumps with electric heating, ensuring stable flow and precise temperature control. A heat exchanger was installed directly before the spinneret to allow fine regulation of the spinning solution temperature and, consequently, more accurate control over the spinning process. The polymer solution was introduced into the coagulation bath through the air gap. The temperature of the coagulation bath was adjustable within the range of 20 to 90 °C, allowing precise control over the amount of water vapor in the air gap. After coagulation, the formed fiber was guided into a washing bath to remove residual solvent and unconsolidated components. Subsequently, the fiber was wound onto a take-up drum with a perimeter of 1.2 meters under continuous water rinsing. Thus, in addition to the standard parameters of non-solvent-induced phase separation, it was possible to control the temperature of the polymer solution relative to its gelling point, as well as the amount of water vapor above the coagulation bath, both influencing the pore distribution within the selective layer.

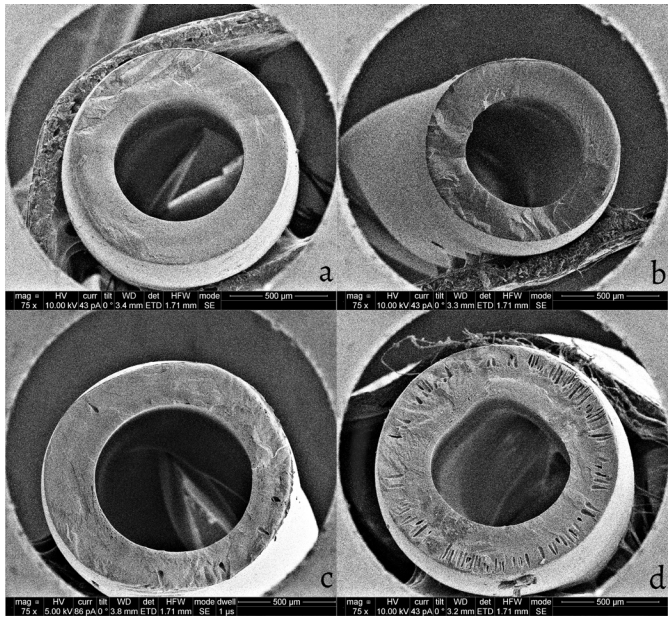

Figure 2: Dependence of macrovoids on the ratio of PVDF Kynar® G150: Solef® 6008*: a) 15:3; b) 12:6; c) 9:9; d) 6:12. *The content of other components was: PVP K90-6%; LiCl-5%; H2O-3.6%; DMSO-27.9%; DMFA-39.5%.

Table 2: Components of the spinning solution.

Components of the spinning solution	PVDF-1	PVDF-3	PVDF-6	PVDF-6_1	PVDF-6_3
	Mass fraction of the component (%)				
KYNAR® G150	12	12	12	12	12
Solef® 6008	6	6	6	6	6
PVP K90	1	3	6	6	6
LiCl	5	5	5	5	5
DMSO	27.6	27.7	27.9	27.9	28
DMFA	44.5	42.5	39.5	38.5	36.5
H20	3.9	3.8	3.6	3.6	3.5
PAR-PAO	-	-	-	1	3

Table 3: Viscosity and gelation temperature of the spinning solutions.

Solution №	T gel, °C	Viscosity at 60°C, Pa*sec
PVDF-1	39	6.9
PVDF-3	42	12.3
PVDF-6	45	18.2
PVDF-6_1	45	19.1
PVDF-6_3	46	19.9

The morphology of the membrane with external selective dry-wet spinning is significantly influenced by the height of the air gap, the composition of the coagulation bath, and the temperature of the coagulation bath. The bore liquid must be mild enough to ensure high porosity without limiting the membrane's permeability. In all cases, the bore composition was 65% DMSO/35% H_2O, rather mild, but at the same time, providing the necessary precipitation rate for stable fiber formation.

The outer selective membrane layer in the air gap is primarily formed by the vapor of the coagulation bath liquid. The use of more volatile and softer precipitants than water, such as isopropyl alcohol, can increase the porosity of the outer selective layer **[32]**. However, for the membrane formation process, reverse osmosis (RO) water was used in the coagulation bath to ensure the process was both eco-friendly and commercially feasible. The porosity and pore size of the selective layer were controlled by adjusting the coagulation bath temperature and the height of the air gap.

The spinneret had the following real dimensions: 1.35 mm—the outer diameter of the outer channel; 0.8 mm—the outer diameter of the bore; and 0.3 mm—the inner diameter of the bore needle. Fibers were formed with a final geometry of 1.3 × 0.75 mm at a take-up speed of 11–12 m/min. The constant spinning parameters are summarized in **Table 4**, while the different hollow fiber fabrication modes are detailed in **Table 5**.

3.3. Post-Processing of the Membrane

After membrane formation, the fibers were kept in reverse osmosis water for 12 hours to remove any residual solvents from the membrane structure. Subsequently, the fibers were transferred to a 5% hydrogen peroxide solution at 60 °C for 12 hours. After this period, the hydrogen peroxide solution was replaced, and the fibers were stored in the fresh solution for another 12 hours at 60°C. This process was repeated a third time for an additional 12 hours. The purpose of this treatment was to remove residual PVP, as it is well known that oxidants such as hydrogen peroxide break down the PVP molecule, significantly accelerating its removal from the membrane **[33]**, while hydrogen peroxide does not have any destructive effects on PVDF.

Finally, the membranes were immersed in a 35% glycerol solution for impregnation and to prevent pore collapse during drying. Drying was carried out using dehydrated air at a temperature of 40°C. The fiber bundles were then filled into mini-modules with a polyurethane compound to check the membrane's cut-off performance.

Table 4: Constant spinning parameters.

Parameter	Value
Coagulation bath composition	H_2O
Bore composition	65/35 DMSO/H_2O
Outer/Inner fiber diameter, mm	1.3/0.75
Take-up speed, m/min	11-12
Polymer solution flow rate, g/min	20
Bore liquid flow rate, g/min	7.5

Table 5: Hollow fiber spinning modes.

Spinning mode №	Air gap, cm	T coagulation bath, °C	T spinneret, °C
A	20	40	40
B	40	40	40
C	60	40	40
D	60	25	40
E	60	60	40
F	60	25	25
G	60	25	60

3.4. Membrane Characteristics

3.4.1. Morphology of the Membrane

As anticipated, the presence of macrovoids in the membrane structure decreased with increasing PVP K-90 concentration in the spinning solution. In the case of the PVDF-1 solution, large macrovoids were present, occupying almost the entire membrane wall. For the PVDF-3 solution, the number of macrovoids was significantly reduced, and no macrovoids were observed in the PVDF-6 fibers **(Figure 3)**. PVP delays the diffusion of solvents from the membrane, leading to the formation of a spongy structure.

The introduction of an amphiphilic block copolymer resulted in a decrease in the pore size of the outer selective layer, confirming the hypothesis that such block copolymers tend to concentrate on the fiber surface **(Figure 4)**. This behavior suggests that block copolymers play a significant role in modifying the membrane's selective layer properties by reducing pore size and enhancing surface structure **(Figure 5)**.

When the height of the air gap above the coagulation bath was reduced to less than 60 cm, the inner opening of the fiber lost its concentricity. This loss of concentricity can be attributed to the viscoelastic properties of PVDF **(Figure 6)**. Rapid phase inversion prevents the relaxation of polymer chains, leading to internal stresses in the nascent hollow fiber that can cause structural disturbances. By increasing the air gap, the contact time between the nascent membrane and the bore liquid was extended, which helped suppress these internal disturbances and maintain the fiber's concentricity.

An increase in the temperature of the coagulation bath resulted in a larger pore size in the outer selective layer **(Figure 7)**. Since the outer layer forms primarily in the air gap under the influence of solvent vapors from the coagulation bath (in

this case, water), raising the bath temperature increased the number of pores in the near-fiber space, leading to a more typical surface pore structure **(Figure 8)**.

The inner surface morphology of the fiber remained consistent across spinning modes, as it was entirely determined by the composition of the coagulation bath. At a spinneret temperature of 60°C, single voids were observed in the fiber structure. This can be attributed to the fact that at this temperature, the solution was sufficiently far from the binodal line, allowing for a substantial outflow of solvent, which initiated the formation of macrovoids **(Figure 9)**. In contrast, at spinneret temperatures of 40°C and 25°C, no macrovoids were observed, and the membrane exhibited a classical spongy structure.

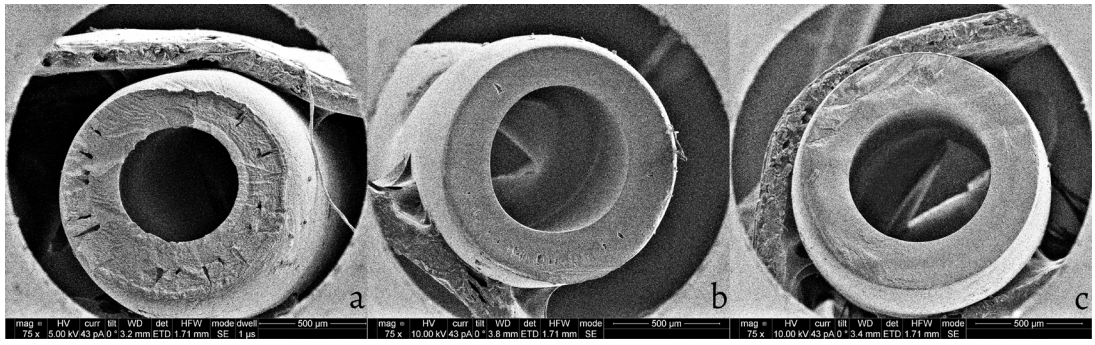

Figure 3: Influence of PVP concentration on hollow fiber morphology: a) 1%; b) 3%; c) 6%; (spinning mode: air gap - 60 cm, T coagulation bath - 25°C, T spinneret - 40°C).

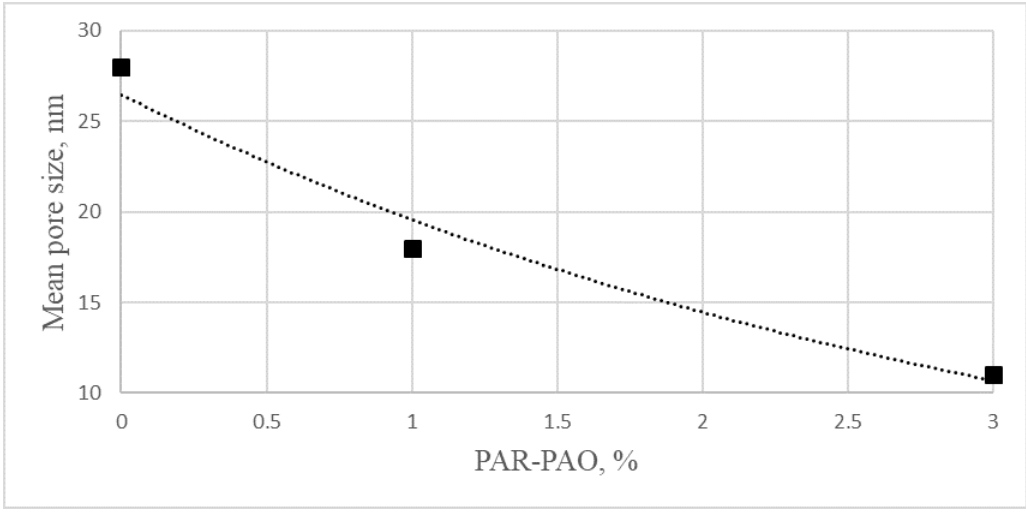

Figure 4: Influence of PAR-PAO on mean pore size (nm).

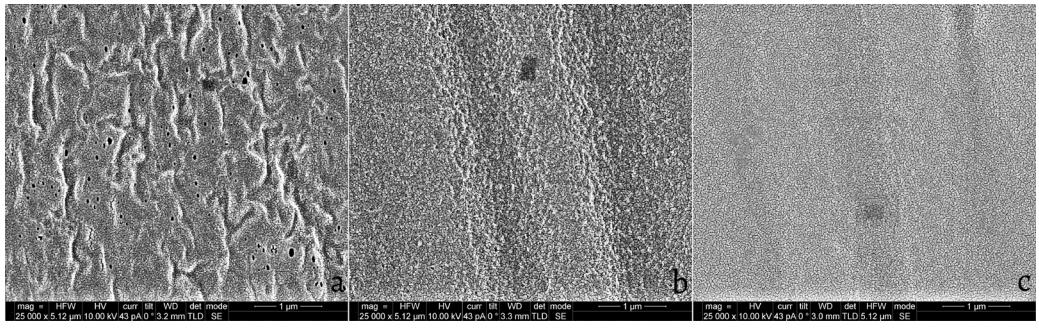

Figure 5: Influence of PAR-PAO on outer layer of hollow fiber: a) 0%; b) 1%; c) 3% (spinning mode: air gap - 60 cm, T coagulation bath - 25°C, T spinneret - 40°C).

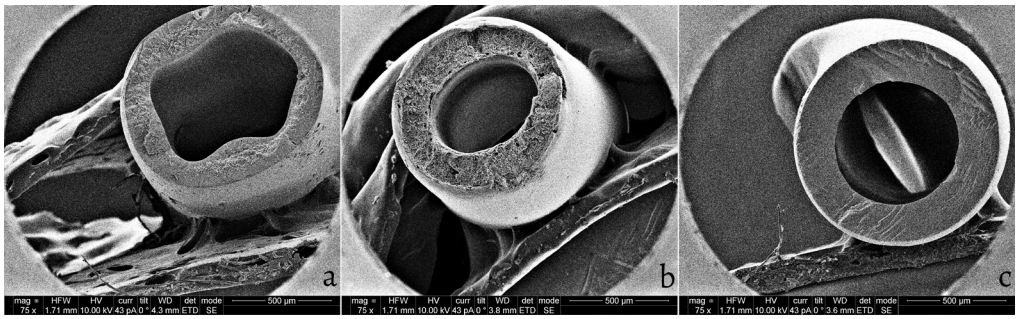

Figure 6: Influence of the air gap on the cross-section of the membrane: a) 20 cm; b) 40 cm; c) 60 cm (spinning solution: PVDF-6).

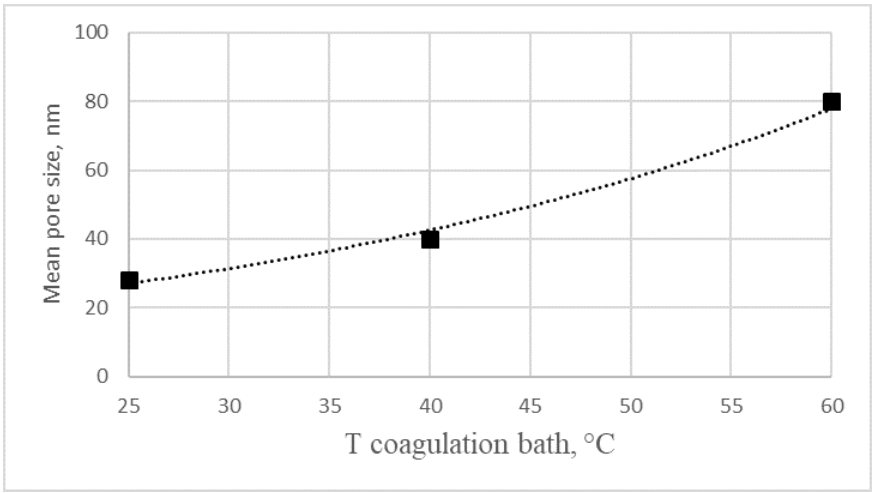

Figure 7: Influence of coagulation bath temperature on mean pore size (nm).

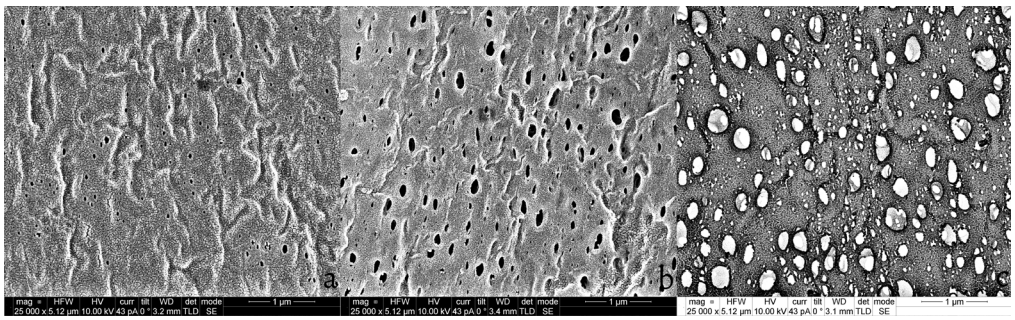

Figure 8: Influence of coagulation bath temperature on the membrane outer layer: a) 40°C; b) 25°C; c) 60°C (spinning solution: PVDF-6).

3.4.2. Membrane Characteristics

Membrane samples were tested for permeability, bubble point, porometry, and protein molecule cut-off (myoglobin, albumin). The tests were conducted exclusively on concentric fibers with a spongy structure. Additionally, for the PVDF-6_1 and PVDF-6_3 formulations, spinnings were carried out only in a 25°C coagulation bath, as amphiphilic block copolymers were used to reduce surface pore size. Higher coagulation bath temperatures would have the opposite effect, which is why combining these two factors was considered inadvisable.

All properties were evaluated after the membranes underwent treatment with a hydrogen peroxide solution and drying using a water–glycerol mixture **(Table 6)**. The observed decrease in permeability and average pore size, along with an increase in albumin cut-off from the PVDF-6(E) to PVDF-6(C) and PVDF-6(D) samples, was expected. This can be attributed to a reduction in the water vapor content in the near-fiber space during molding at lower bath temperatures. When the spinneret temperature was reduced to 25°C (PVDF-6(F) sample), membrane permeability decreased, while other fiber characteristics remained largely unchanged. This phenomenon can be attributed to the fact that, at temperatures below the gel point, the solid–liquid phase separation process predominates, leading to the formation of spherulites with a closed, low-permeable structure. As a result, the membrane's porosity decreases, though the size of the limiting pore remains unaffected. Similar behavior was observed when comparing the PVDF-6_1(D) and PVDF-6_1(F) samples, as well as the PVDF-6_3(D) and PVDF-6_3(F) samples **(Figure 10)**.

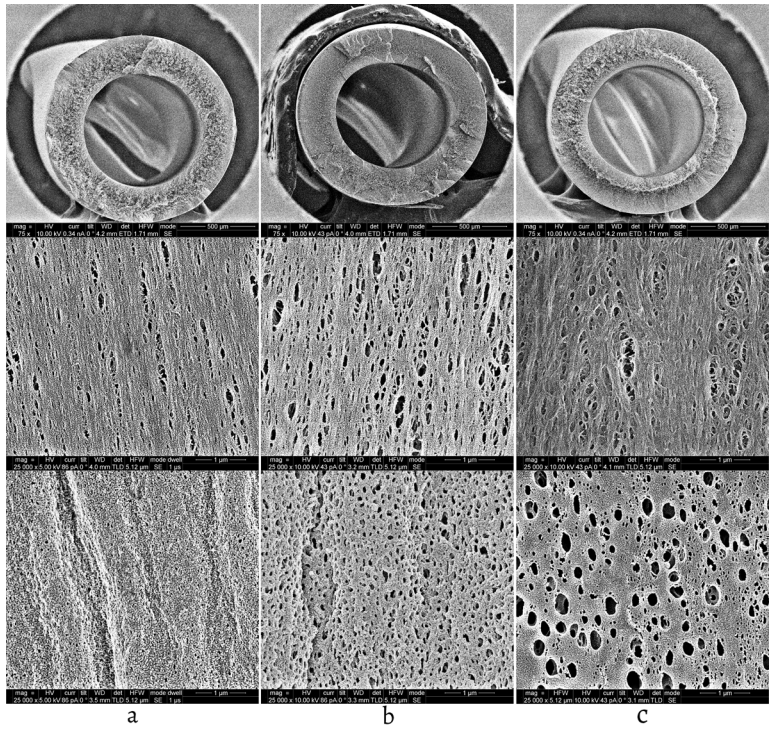

Figure 9: Influence of spinneret temperature on the membrane morphology: a) 25°C; b) 40°C; c) 60°C (spinning solution: PVDF-6).

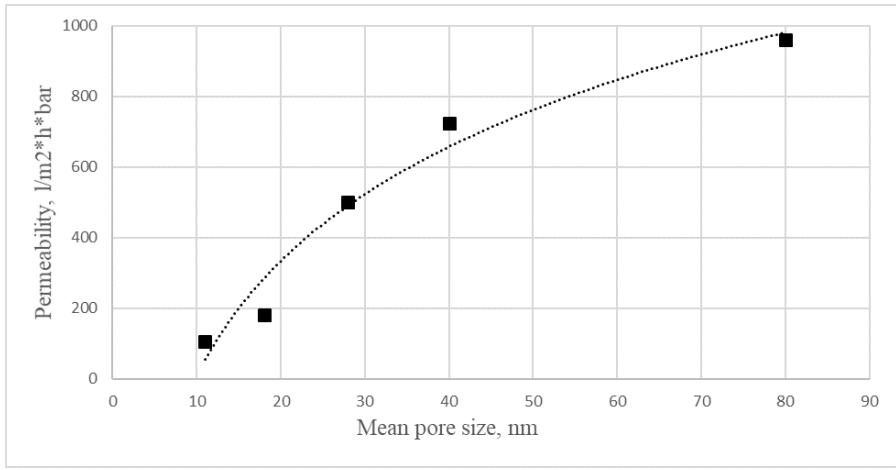

Figure 10: Dependence of permeability of hollow fiber membranes on pore size for PVDF.

Table 6: Membrane characteristics.

Solution № (spinning mode №)	Permeability, l/ m^2*h*bar	Albumin cut-off (%)	Myoglobin cut-off (%)	Bubble point in H_2O (bar)	Mean pore size (nm)
PVDF-6(E)	960	75	0	6.9	80
PVDF-6(C)	725	90	0	7.0	40
PVDF-6(D)	500	95+	0	7.1	28
PVDF-6(F)	370	95+	0	7.0	29
PVDF-6_1(F)	180	95+	45	7.3	18
PVDF-6_1(D)	310	95+	48	7.2	18
PVDF-6_3(F)	68	95+	95+	7.5	10
PVDF-6_3(D)	105	95+	95+	7.5	11

None of the PVDF-6 membrane samples exhibited a myoglobin cut-off. Without the addition of amphiphilic block copolymers, it was impossible to achieve a 20 kDa cut-off. However, fibers made from the PVDF-6_1 and PVDF-6_3 compositions had sufficiently small limiting pores to demonstrate a myoglobin cut-off. As expected, an increase in PAR-PAO concentration led to a decrease in membrane permeability, and the cut-off value shifted toward higher molecular weights. Fibers containing PAR-PAO exhibited slightly higher bubble point values, suggesting that the block copolymer may positively influence the mechanical properties of the membrane.

4. Conclusions

This study demonstrated that the composition of the spinning solution and the processing conditions have a profound effect on the morphology and performance of PVDF-based hollow fiber membranes. The use of two distinct PVDF grades with different molecular weights, KYNAR® G150 and Solef® 6008, showed that higher molecular weight PVDF contributed to enhanced mechanical strength, while the lower molecular weight PVDF facilitated the reduction of solution viscosity, leading to smoother membrane surfaces and improved permeability.

The incorporation of additives such as polyvinylpyrrolidone (PVP K-90) and lithium chloride (LiCl) significantly influenced the final membrane structure. Increasing the PVP concentration resulted in a reduction of macrovoids and an increase in porosity, enhancing the overall hydrophilicity of the membrane. Furthermore, the use of amphiphilic block copolymers, specifically polyarylate-polyalkylene oxide (PAR-PAO), effectively controlled the pore size of the outer selective layer, thereby improving the selectivity of the membrane.

Temperature control during the coagulation and spinning processes was also crucial. The temperature of the coagulation bath influenced the pore size of the outer selective layer, with higher temperatures promoting larger pores. In contrast, spinneret temperature affected macrovoid formation—higher temperatures shifted the solution further from the binodal line, while lower temperatures (25°C) favored solid-liquid phase separation, resulting in lower membrane permeability due to the formation of a closed, low-permeability structure.

The results confirm that by adjusting the spinning solution components and processing conditions, it is possible to tailor the structural and functional properties of PVDF hollow fiber membranes. By adjusting the coagulation bath temperature and the PAR-PAO block copolymer content in the spinning solution, membranes with the desired selective pore size can be obtained while maintaining a regular spongy structure.

Acknowledgments

We would like to thank Prof. Storozhuk P. Ivan for his assistance in synthesizing PAR-PAO-type block copolymers. We also extend our gratitude to Kukueva V. Elena for creating the SEM images.

Authors' Contribution

Conceptualization, NF; methodology, KV; formal analysis, AK and GK; Writing—original draft preparation, NF, AD, and TY; Writing—reviewing and editing, MI. All authors have read and agreed to the published version of the manuscript.

Data Availability Statement

The data supporting the findings of this study are available upon request from the corresponding author.

Funding

This research received no external funding.

Conflicts of Interest

The authors declare no conflicts of interest to be disclosed.

Declaration of Generative AI and AI-Assisted Technologies

In preparing this work, the author used Chat GPT to ensure a clear translation into English. After using this service, the author reviewed and edited the content as needed and takes full responsibility for the content of the publication.

References

[1] Mulder M. Basic principles of membrane technology. Dordrecht: Springer Netherlands; 1991. https://doi.org/10.1007/978-94-017-0835-7.

[2] Guillen GR, Pan Y, Li M, Hoek EMV. Preparation and characterization of membranes formed by Nonsolvent induced phase separation: a review. Industrial & Engineering Chemistry Research 2011;50:3798–817. https://doi.org/10.1021/ie101928r.

[3] Fontananova E, Bahattab MA, Aljlil SA, Alowairdy M, Rinaldi G, Vuono D, *et al*. From hydrophobic to hydrophilic polyvinylidenefluoride (PVDF) membranes by gaining new insight into material's properties. RSC Advances 2015;5:56219–31. https://doi.org/10.1039/c5ra08388e.

[4] Zhang B, Ma S. Study on fouling and cleaning of PVDF membrane. Modern Applied Science 2009;3:25. https://doi.org/10.5539/mas.v3n11p52.

[5] Liu F, Hashim NA, Liu Y, Abed MRM, Li K. Progress in the production and modification of PVDF membranes. Journal of Membrane Science 2011;375:1–27. https://doi.org/10.1016/j.memsci.2011.03.014.

[6] Kang G, Cao Y. Application and modification of poly(vinylidene fluoride) (PVDF) membranes – A review. Journal of Membrane Science 2014;463:145–65. https://doi.org/10.1016/j.memsci.2014.03.055.

[7] Abed MRM, Kumbharkar SC, Groth AM, Li K. Ultrafiltration PVDF hollow fibre membranes with interconnected bicontinuous structures produced via a single-step phase inversion technique. Journal of Membrane Science 2012;407–408:145–54. https://doi.org/10.1016/j.memsci.2012.03.029.

[8] Fontananova E, Jansen JC, Cristiano A, Curcio E, Drioli E. Effect of additives in the casting solution on the formation of PVDF membranes. Desalination 2006;192:190–7. https://doi.org/10.1016/j.desal.2005.09.021.

[9] Wang D, Li K, Teo WK. Preparation and characterization of polyvinylidene fluoride (PVDF) hollow fiber membranes. Journal of Membrane Science 1999;163:211–20. https://doi.org/10.1016/s0376-7388(99)00181-7.

[10] Chang H-H, Chen S-C, Lin D-J, Cheng L-P. The effect of Tween-20 additive on the morphology and performance of PVDF membranes. Journal of Membrane Science 2014;466:302–12. https://doi.org/10.1016/j.memsci.2014.05.011.

[11] Cao X, Ma J, Shi X, Ren Z. Effect of TiO2 nanoparticle size on the performance of PVDF membrane. Applied Surface Science 2006;253:2003–10. https://doi.org/10.1016/j.apsusc.2006.03.090.

[12] Lee GM, Choi DC, Seo CM. Composition for membrane, method of preparing membrane using the same, membrane prepared therefrom and apparatus for purifying water. US20180085715A1, 2018.

[13] Du C-H, Wu C-J, Wu L-G. Effects of pluronic F127 on the polymorphism and thermoresponsive properties of PVDF blend membranes via immersion precipitation process. Journal of Applied Polymer Science 2012;124:E330–7. https://doi.org/10.1002/app.35257.

[14] Lin D, Beltsios K, Chang C, Cheng L. Fine structure and formation mechanism of particulate phase-inversion poly(vinylidene fluoride) membranes. Journal of Polymer Science Part B: Polymer Physics 2003;41:1578–88. https://doi.org/10.1002/polb.10513.

[15] Fateev NN, Yasneva TA, Kustlivy IK, Ivanov MV, Kagramanov GG. Preparation of TFC-PES reverse osmosis hollow fibre membrane for brackish water desalination. Journal of Advanced Research in Fluid Mechanics and Thermal Sciences 2024;119:13–27. https://doi.org/10.37934/arfmts.119.1.1327.

[16] Vroman T. Mechanisms of hollow-fiber membrane fouling removal used in water treatment : critical backwash fluxes and membrane deformation for an enhanced backwash efficiency. phdthesis. Université Paul Sabatier - Toulouse III, 2020.

[17] Deshmukh SP, Li K. Effect of ethanol composition in water coagulation bath on morphology of PVDF hollow fibre membranes. Journal of Membrane Science 1998;150:75–85. https://doi.org/10.1016/s0376-7388(98)00196-3.

[18] Dehban A, Hosseini Saeedavi F, Kargari A. A study on the mechanism of pore formation through VIPS-NIPS technique for membrane fabrication. Journal of Industrial and Engineering Chemistry 2022;108:54–71. https://doi.org/10.1016/j.jiec.2021.12.023.

[19] Tanis-Kanbur MB, Peinador RI, Calvo JI, Hernández A, Chew JW. Porosimetric membrane characterization techniques: a review. Journal of Membrane Science 2021;619:118750. https://doi.org/10.1016/j.memsci.2020.118750.

[20] Mkheidze N, Gotsiridze R, Mkheidze S, Pattyn D. Determination of the polymeric membranes pore size distribution by the method of capillary flow porometry 2020;14:64–71.

[21] Haponska M, Trojanowska A, Nogalska A, Jastrzab R, Gumi T, Tylkowski B. PVDF membrane morphology—influence of polymer molecular weight and preparation temperature. Polymers 2017;9:718. https://doi.org/10.3390/polym9120718.

[22] Tuncay G, Türken T, Koyuncu İ. Investigation of different molecular weight Polyvinylidene Fluoride (PVDF) polymer for the fabrication and performance of braid hollow fiber membranes. Environmental Technology 2022;45:404–17. https://doi.org/10.1080/09593330.2022.2112092.

[23] Marshall JE, Zhenova A, Roberts S, Petchey T, Zhu P, Dancer CEJ, *et al*. On the solubility and stability of polyvinylidene fluoride. Polymers 2021;13:1354. https://doi.org/10.3390/polym13091354.

[24] Lee J, Park B, Kim J, Park SB. Effect of PVP, lithium chloride, and glycerol additives on PVDF dual-layer hollow fiber membranes fabricated using simultaneous spinning of TIPS and NIPS. Macromolecular Research 2015;23:291–9. https://doi.org/10.1007/s13233-015-3037-x.

[25] Mıyano T, Matsuura T, Sourirajan S. Effect of polyvinylpyrrolidone additive on the pore size and the pore size distribution of polyethersulfone (Victrex) membranes. Chemical Engineering Communications 1993;119:23–39. https://doi.org/10.1080/00986449308936105.

[26] Chakrabarty B, Ghoshal AK, Purkait MK. Preparation, characterization and performance studies of polysulfone membranes using PVP as an additive. Journal of Membrane Science 2008;315:36–47. https://doi.org/10.1016/j.memsci.2008.02.027.

[27] Yoo SH, Kim JH, Jho JY, Won J, Kang YS. Influence of the addition of PVP on the morphology of asymmetric polyimide phase inversion membranes: effect of PVP molecular weight. Journal of Membrane Science 2004;236:203–7. https://doi.org/10.1016/j.memsci.2004.02.017.

[28] Fateev N, Ivanov M, Korotkova N, Dibrov G, Pavlukovich N, Storozhuk I. Influence of additives of amphiphilic block copolymers on the porosity of hollow ultrafiltration membranes based on polyethersulfone. E3S Web of Conferences 2023;376:01022. https://doi.org/10.1051/e3sconf/202337601022.

[29] Espinosa-Dzib A, Vyazovkin S. Gelation of poly(vinylidene fluoride) solutions in native and organically modified silica nanopores. Molecules 2018;23:3025. https://doi.org/10.3390/molecules23113025.

[30] Ma W, Cao Y, Gong F, Liu C, Tao G, Wang X. Poly(vinylidene fluoride) membranes prepared via nonsolvent induced phase separation combined with the gelation. Colloids and Surfaces A: Physicochemical and Engineering Aspects 2015;479:25–34. https://doi.org/10.1016/j.colsurfa.2015.04.004.

[31] Dibrov G, Ivanov M, Semyashkin M, Sudin V, Fateev N, Kagramanov G. Elaboration of high permeable Macrovoid free polysulfone hollow fiber membranes for air separation. Fibers 2019;7:43. https://doi.org/10.3390/fib7050043.

[32] Basko A, Lebedeva T, Yurov M, Ilyasova A, Elyashevich G, Lavrentyev V, *et al*. Mechanism of PVDF membrane formation by nips revisited: effect of precipitation Bath nature and polymer–solvent affinity. Polymers 2023;15:4307. https://doi.org/10.3390/polym15214307.

[33] Loraine GA. Oxidation of polyvinylpyrrolidone and an ethoxylate surfactant in phase-inversion wastewater. Water Environment Research 2008;80:373–9. https://doi.org/10.2175/106143008x266779.

How to Cite

Fateev N, Velmozhin K, Danilkin A, Kotyukova A, Yasneva T, Ivanov M, et al. Enhanced Filtration Performance of Hollow Fiber PVDF Membranes with Selective Pore Size Control via Modified NIPS Method. Membrane Sci Int 2025;4(1):1–11.